Climate Services 43 (2026) 100668

Contents lists available at ScienceDirect

Climate Services

journal homepage: www.elsevier.com/locate/cliser

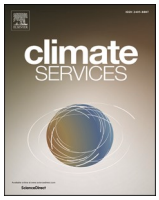

Simulation of subnational projections of poverty and income distribution to support climate risk assessments: A case-study for Ethiopia

Michiel van Dijk [a,b,*], Marijke Kuiper [a], Thijs de Lange [a], Jason F.L. Koopman [a], Willem-Jan van Zeist [a]

[a] Wageningen Social & Economic Research, Wageningen University & Research (WUR), Prinses Beatrixlaan 582-528, 2595 BM, the Hague, the Netherlands
[b] International Institute for Applied Systems Analysis (IIASA), Schlossplatz 1, A-2361, Laxenburg, Austria

HIGHLIGHTS

- This study presents a novel spatial microsimulation modelling framework to assess the vulnerability of the poor to extreme climate events.
- The framework was applied to determine the number, demographic characteristics and occupation of the poor population in Ethiopia that are exposed to heat stress under various socio-economic and climate scenarios.
- We found that between 1.4 and 9.4 million poor people in Ethiopia will be at risk of extreme heat in 2050.
- The approach can be extended to include a variety of climate hazard and can be applied to other countries and regions.

ABSTRACT

The global poor are expected to suffer most from the impact of climate change, in particular the increasing frequency of extreme weather events. To develop targeted climate adaptation strategies, national decision makers need to have detailed information on the quantity, location and profile of the people that are most vulnerable to climate hazards. This study presents an innovative spatial microsimulation modelling framework for projecting subnational income distribution and poverty trends under different scenarios that can be combined with spatial data on climate hazards to support climate risk assessments. The model combines household survey data with subnational projections on key drivers of income to simulate how the distribution of income changes as a consequence of economic development and structural transformation. To illustrate our modelling framework, we provide an application to Ethiopia. We projected changes in poverty headcount and income distribution for 60 different zones and three different socio-economic scenarios for the period 2020–2050. We combined the subnational income projections with heat stress maps to identify the number and profile of the population that are most vulnerable to climate change and found that, depending on the scenario, between 1.4 and 9.4 million poor people (1-5% of the population) will be at risk of heat stress in Ethiopia in 2050. The modelling framework can be combined with spatial data of additional climate hazards, such as floods and droughts, and be applied to other countries and regions, to support national climate information systems and inform climate adaptation strategies and policies.

Practical implications

Detailed information on the location and exposure of population groups to climate hazards are essential for climate risk assessments and the formulation of national policies and long-term climate adaptation plans. In particular, it is important to know the location and profile of the poor, which are among the most vulnerable to climate hazards because they have limited financial means to cope with shocks and are often hit the hardest because of their dependence on agriculture for food and income (Hallegatte et al., 2016).

The majority of existing climate risk assessments combine population projections (Ward et al., 2020) or historical poverty maps (Adshead et al., 2024; Rentschler et al., 2022) with spatially explicit information on future hazards to determine the share of the population at risk. None of these studies provide guidance on the exposure of the future poor to the impact of expected climate extremes. Recent geopolitical tensions and conflicts illustrate that economic development is highly uncertain and global shocks might have dramatic impact on future income distribution and poverty. It is important to account for these uncertainties in climate risk assessments.

* Corresponding author at: Wageningen Social & Economic Research, 2595 BM, the Hague, the Netherlands.
E-mail address: michiel.vandijk@wur.nl (M. van Dijk).

https://doi.org/10.1016/j.cliser.2026.100668
Received 3 June 2025; Received in revised form 11 April 2026; Accepted 12 May 2026
Available online 22 May 2026

This paper presents a spatial microsimulation modelling framework that creates small area income distribution and poverty projections using a bottom-up approach based on different socio-economic scenarios. The results can be combined with spatial datasets that provide information on the location and intensity of climate hazards to identify high-risk hotspots where high-poverty levels overlap with the location of extreme weather events.

We present a case-study in which we use the modelling approach to assess the vulnerability and profile of the poor in Ethiopia to heat stress. The analysis points at the existence of several poverty-climate hotspots. Given the limited capacity of the poor to protect themselves from heat stress, heat-related illness, mortality and reductions in labor productivity will be high in these areas unless preventive measures are taken. Such measures may include developing heat action plans that improve public awareness and promote adaptive measures, setting up early warning systems that give the population timely information about heat waves and investigating possibilities to change working hours in agriculture and construction, where workers are most vulnerable to heat stress.

The climate risk analysis can be extended by combining the results with projections for floods and droughts, which, in addition to the heat related climate hazards, are regarded as the main climate hazards in Ethiopia (Conway and Schipper, 2011) and other climate extremes. Such information will be useful input for the development and refinement of national adaptation plans and the Ethiopia Nationally Determined Contributions (NDC) that describe and prioritize strategies to adapt to climate change. Interestingly, the latest Ethiopian NDC (Federal Democratic Republic of Ethiopia, 2021), which includes a detailed list of adaptation actions, does not identify heat stress as a priority, nor does it provide any details on regional measures and risks related to climate adaptation. The results of the spatially explicit climate risk assessment presented in this paper, could be used to improve and deepen the next iteration of the Ethiopian NDC.

The modelling approach is flexible enough to be run at different scales and incorporate alternative scenario assumptions that are often prepared as part of participatory modelling exercises to inform climate risk assessments (Merkle et al., 2023). To support decision making at the local level, one option would be to apply the modelling framework to a subset of selected districts for which detailed input data can be collected in combination with stakeholder proposed scenarios. The main input for the model are global datasets (e.g. national population and labor statistics) and spatial layers (e.g. urbanization and demographic maps and projections), which are publicly available, as well as a national household income and expenditure survey, which often can be sourced from national statistics. For this reason, our approach can relatively easily be extended to other countries and regions. Policy makers can use the model as part of a national climate information system to inform climate adaptation strategies and policies.

Introduction

There is abundant evidence that poor countries and poor people will suffer most from climate change (Diffenbaugh and Burke, 2019; Hallegatte et al., 2016; Hsiang et al., 2017; Sedova et al., 2019). Poor people are the most vulnerable to climate-related extremes and hazards, such as floods, droughts and extreme heat because they have limited financial means to cope with shocks. In addition, the poor often rely heavily on agriculture as their primary source of income, making them disproportionately affected by climate-related disruptions to agricultural activities and have limited access to necessities such as food, water and healthcare, which might worsen under climate change (Hallegatte and Rozenberg, 2017). A recent study estimated that without further action, climate change impacts could push more than 130 million into poverty by 2030 (Jafino et al., 2020).

To formulate climate adaptation strategies and interventions, decision makers conduct climate risk assessments to identify which part of the population has the highest risk to be negatively affected by climate-related shocks and what measures are needed to protect the most vulnerable segment of the population and increase their resilience. To determine the human risk from climate impacts, information on three dynamically interacting components is required (IPCC, 2022): (a) the probability of climate-related hazard; (b) the exposure of the population to a hazard and (c) the vulnerability of the population to a hazard.

In recent years there has been an increasing availability of high-resolution spatial datasets that present information on the probability and location of climate-related hazards under different socio-economic and climate scenarios, including sea level rise (Kirezci et al., 2020), floods (WRI, 2020), droughts (Satoh et al., 2022) and heat stress (Schwingshackl et al., 2021). A number of studies used this information to assess current and future exposure to extreme climate events at various scales (Lange et al., 2020; Osberghaus and Abeling, 2022; Rising et al., 2022; Strauss et al., 2021). However, most studies (Ward et al., 2020) only combine population maps with spatially explicit information on hazards to determine the share of the population at risk. Therefore, they do not provide a complete climate risk assessment as vulnerability is not taken into account.

Another strand of research provides projections of human vulnerability under different socio-economic and climate scenarios to better analyze the impact of climate change on social well-being. In these studies, vulnerability is measured by income distribution and poverty indicators (Rao et al., 2019; Soergel et al., 2021) or by more advanced composite indices that also include education and food security indicators (Liu et al., 2024; Marzi et al., 2025). These studies mostly have a national-level focus and do not provide results on the spatial distribution of vulnerability within a country.

Recent studies by Rentschler et al. (2022) and Adshead et al. (2024) addressed this issue and combined projections of climate hazards with spatial poverty estimates to assess the climate vulnerability at higher spatial resolution. However, they used historical poverty maps to determine the location of the poor and therefore do not take into account the impact of different socio-economic development trajectories on income and poverty change. Both COVID and current geopolitical tensions and conflicts have shown that the future is highly uncertain and global shocks can have a dramatic impact on future socio-economic development and global poverty (Mahler et al., 2022), thereby affecting the future vulnerability and risk of climate shocks. This implies that the preparation of comprehensive climate risk assessments requires a scenario approach that combines high-resolution climate hazard projections with spatially explicit estimations of future poverty, which is considered as a reasonable proxy for vulnerability (Rana et al., 2023).

The aim of this paper is to fill this gap and to demonstrate a modelling framework that creates small area income distribution and poverty projections using a bottom-up approach based on different socio-economic scenarios. Such maps can be combined with spatial datasets that provide information on the location and intensity of climate-hazards to identify high-risk hotspots where extreme weather events overlap with the location of the most vulnerable segment of the population. This paper presents the Microsimulation of Income DynamicS (MIDS) model, which combines spatial microsimulation with inputs from a global economic simulation model and assumptions that are consistent with the shared-socioeconomic pathways (SSPs), the dominant scenario framework for climate assessments (Riahi et al., 2017; van Vuuren et al., 2017). As such, it aims to bridge the scales between (a) climate impact and vulnerability research, which requires data with detailed spatial resolution, and (b) integrated assessment modelling, which mainly uses macro-level approaches to simulate change in socio-economic indicators (van Ruijven et al., 2014; Soergel et al., 2021). Our approach can be regarded as a first step to improve spatial heterogeneity and distributional effects in climate change scenario modelling to support the development of local adaptation and

mitigation strategies. This has been identified as a key priority for future climate risk and scenario research (Piontek et al., 2021; Pirani et al., 2024; Rao et al., 2017).

To illustrate the modelling framework we provide an application for Ethiopia, one of Africa's most populous countries, which also experiences high levels of poverty. Climate projections for Ethiopia predict rising temperatures and a greater frequency of heat waves (Conway and Schipper, 2011), which are expected to have severe negative effects on agriculture, poverty and child stunting (Berhanu et al., 2024; Mideksa, 2010; Randell et al., 2020). We used the narratives and (gridded) quantified drivers of the SSPs to generate projections of demographic change, urbanization and occupation across 60 zones in Ethiopia. In addition, we extended the standard SSP assumptions, which are limited to the national scale, with spatial and micro-level assumptions that are consistent with the SSP storylines. These are subsequently used in the MIDS model to create poverty maps for different scenarios. Finally, we conducted a climate risk assessment by combining the poverty maps with heat stress projections for different climate scenarios to identify vulnerability hotspots and provide information on the age, occupation and urban–rural profile of the people most vulnerable to future extreme hot weather.

Methods and materials

Conceptual framework

Long-run income changes at the household level are the outcome of a complex interaction of local (e.g. demography and degree of urbanization), national (e.g. structural transformation of the economy and redistributive policies) and global (e.g. climate change, trade, pandemics and wars) driving forces (Acemoglu et al., 2002; Burke et al., 2015; Dollar et al., 2016; Mahler et al., 2022). To capture these factors, the MIDS model, combines spatial microsimulation (Tanton and Edwards, 2013) with micro–macro simulation approaches (see Bourguignon and Bussolo (2013) and van Ruijven et al. (2015) for reviews) to project income distribution and income change at the subnational level.

Spatial microsimulation is a method to model and analyze population dynamics at a small geographic scale, such as districts, municipalities and provinces. It involves combining household level information from surveys with aggregate population and demographic statistics (referred to as 'constraint' variables) from a population census to derive household weights that reproduce the characteristics of the actual population in a small area (Lovelace and Dumont, 2016). The weights are then combined with the survey data to simulate the distribution of the target variable (in this case household income) for that area. Spatial microsimulation has been used to analyze the geographical distribution of poverty, health, transport and housing (Tanton and Edwards, 2013). Spatial microsimulation models are a useful tool to inform regional policies and rural–urban planning as they provide information at spatial levels for which only scarce and fragmented data is available.

To project the spatial distribution of household income distribution over time, MIDS updates both the weight and the income level of each household into the future. The household weights are adjusted in such a way that the (sub)national population totals are consistent with the (sub)national age, sex, occupation and urban–rural projections that are prepared as part of socio-economic scenarios and which can be considered as the main drivers of change in income distribution (see below). To capture the impact of these drivers on the distribution of income, the reweighting procedure gives higher weights to households with characteristics that are projected to become more dominant in the future and lower weights to households with characteristics that are projected to become less dominant. This means that in scenarios which are characterized by structural economic transformation, the reweighting procedure will allocate higher weights to households with members that are active in manufacturing and services in comparison to households that work in agriculture. Similarly, urbanization and aging of the population are simulated by giving higher weights to urban households (relative to rural households) and households with a large share of elderly family members, respectively.

Apart from changes in the composition of the population, which are captured by the reweighting procedure, growth in (subnational) income distribution will also be affected by changes in the level of household income over time. MIDS distinguishes between two channels that affect household income. The first are changes in factor income, in particular from labor, which makes up the largest component of household income in low-income countries, such as Ethiopia. Labor income is shaped by macro-drivers such as technological progress (e.g. farmers using tractors instead of animal traction), changes in the demand for labor (e.g. an increase in the demand for high-skilled labor) and changes in the supply of labor (e.g. a growing or aging population). Similar to micro–macro poverty studies (Ahmed et al., 2020; Bussolo et al., 2010a; Laborde Debucquet and Martin, 2018), MIDS uses the output from a global Computable General Equilibrium (CGE) model (MAGNET) to simulate the impact of macro-drivers on factor income. The advantage of a global simulation model is that it accounts for the impact of global shocks and events, (e.g. trade barriers and climate change impact) that are transmitted through international trade, on national economic development. The second channel that influences household income are policies (e.g taxes, subsidies and pension systems) to redistribute income. To model these, MIDS includes the option to simulate a flat household income tax, which is used to fund a basic income and pensions.

Finally, the updated weights and household income are combined to project the simulated future income distribution and poverty at the spatial level. Fig. 1 depicts the MIDS modelling framework and the two major channels that determine future household income distribution and poverty. The following sections provide detailed information on key components of the MIDS model and the data.

Dynamic spatial microsimulation

The core of MIDS is a dynamic spatial microsimulation approach to account for spatial drivers of household income change over time. More specifically, the model implements a 'pseudo-dynamic' approach (Harding et al., 2011; Tanton, 2014; Vidyattama and Tanton, 2010), which combines a household survey with constraints that are projected into the future. For each period, new household weights were derived using the iterative proportional updating (IPU) algorithm (Ye et al., 2009), which takes into account both household and household member characteristics (Supplementary Section 4).

A key assumption in spatial microsimulation is that the constraints are strong predictors for the variable of interest, in this case household income, for which data is only available in the survey. For our study, we selected five constraint variables: occupation, urban–rural status, age, sex and number of households. Occupation is strongly related to a person's level of education and skill-level at work, which jointly are key drivers of wage and income (de Beyer and Knight, 1989; Gibbons et al., 2005). The distribution of occupations is also related to the process of structural economic transformation in which people move from low-skilled jobs in agriculture to high-skill jobs in manufacturing and services (Duernecker and Herrendorf, 2022; Syrquin, 1988). Accounting for change in the distribution of occupations over time by updating survey weights will capture the impact of structural change on income distribution. We distinguished between five major occupations following the major International Standard Classification of Occupations (ISCO): professionals, technicians, clerks, service workers and agricultural & craft workers (Supplementary Table 1) and three additional classes: elderly (65 years and above), children (under 15 years) and adults not in the labor force (students and adults unable or unwilling to pursue paid work), which together describe the total population.

Urbanization is another important determinant of household income. Several studies describe the existence of a persistent urban–rural wage gap, which is explained by differences in skill level between urban

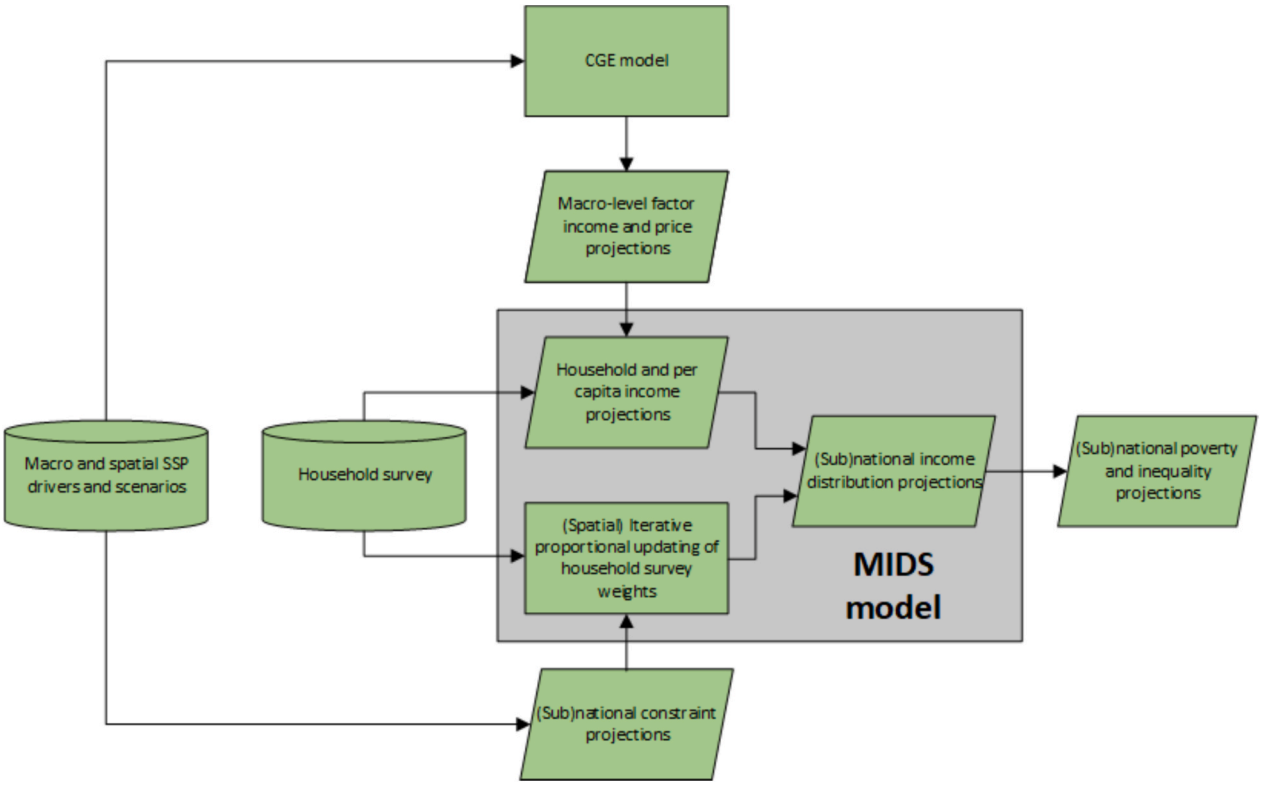

Fig. 1. MIDS modelling framework.

and rural workers (Young, 2013) as well as market failures (Munshi and Rosenzweig, 2016). We used two classes (urban and rural) to incorporate urbanization in the model.

Sex and age are key variables that describe the demographic change of the population. Adding these as constraints captures the impact of differences in income between young and old workers and between male and female workers and how this impacts income distribution as a consequence of demographic change. Including age and sex also ensures consistency between MIDS and population projections, which are a key driver of the macro-simulation model that informs MIDS. We distinguished between two sexes (male and female) and seven age classes. Similar to Hallegatte et al. (2017), we decided to exclude the number of children in a household from the re-weighting procedure and proportionally rescale the number of children (age < 15) per household after the simulation to match the subnational projections for the age class of under 15. The reason for doing this is that the household survey contains a very low number of households with a small number of children, which makes it difficult to calibrate weights for low population growth scenarios.

Finally, to maintain the link between income, which is determined at the household level and demographic change, which is determined by the family member structure, we added the number of households as a constraint in the reweighting procedure.

Macro-drivers of income change

We used macro-level projections for changes in labor income from the MAGNET model to update household-level income information in MIDS. MAGNET is a recursive dynamic global CGE model that includes an improved labor market module to simulate the markets and resulting labor income for each of the five major occupation classes under different future scenario projections. To link the MAGNET income projections to MIDS, we decomposed household income from the survey (approximated by total consumption expenditure) in labor and non-labor contributions using a regression approach (Hallegatte and Rozenberg, 2017). The process involved four steps (see Supplementary Section 5 for details). First, we allocated one of the five major occupation classes to each person in the household, using information from the household survey. Second, we used robust regression, which accounts for the impact of outliers (Andersen, 2008) to estimate the average contribution of each person with a certain occupation to the total labor income of the household. We distinguished between urban and rural populations to control for differences in income sources between both population groups. Third, we combined the estimated coefficients for each occupation class with real labor income change projections from MAGNET and calculated the total labor income for each household in future periods. Finally, we scaled the simulated income distribution in such a way that the change in mean income per capita was consistent with the change in real GDP per capita from the SSP projections. The scaling can be regarded as an adjustment factor to account for the change in capital income, which is not captured by our procedure to update household labor income (Bussolo et al., 2010b).

Household survey data

We used the fourth wave (2018–2019) of the Ethiopia Socio-economic Survey (ESS4) (Central Statistics Agency of Ethiopia, 2020) as a source of household information. The ESS4 is a multi-topic baseline survey that addresses a wide number of socio-economic and demographic variables, including income and consumption. In comparison to the previous waves, the consumption module of ESS4 was revised to ensure it is consistent with the Household Income and Consumption Expenditure Survey (HICES), which is the official source to estimate national poverty statistics. The ESS4 is representative for 11 major regions as well as urban and rural areas. It was conducted in 535 enumeration areas and includes information on 6,770 households. We used the total household consumption expenditure, corrected for spatial variation in food prices that is available in ESS4, as a proxy for household income. A consumption-based measure is considered as a much more reliable source than total income for poor countries (Haughton and

Khandker, 2009) and is therefore used as the preferred indicator to measure poverty (Seff and Jolliffe, 2017; World Bank, 2020). Following standard practices in international poverty analysis (World Bank, 2025), we converted household income into 2017 PPP$ values to make it comparable with the international poverty line and used the change in GDP per capita to project the survey data from 2018 to 2020, the first year of our simulation exercise (see Supplementary Section 2 for details).

Scenarios and subnational projections

As a basis for our projections we used the Shared-Socioeconomic Pathways (SSPs), a set of socio-economic scenarios that were developed for climate change research (Riahi et al., 2017; van Vuuren et al., 2017) but are increasingly used as narratives to guide a range of global assessments (Leclère et al., 2020; Willett et al., 2019). The SSPs consist of five storylines that each describe different future worlds as well as related projections of key drivers (O'Neill et al., 2017). In this study, we limited the analysis to three scenarios: SSP1 (Sustainability), SSP2 (Middle of the road) and SSP3 (Regional rivalry). SSP1 and SSP3 are frequently used in simulation studies because they are regarded as the most extreme socio-economic scenarios, while SSP2 is considered as a business-as-usual or baseline scenario. As the SSP3 narrative does not contain explicit information on intra-country inequality trends, we decided to adopt the SSP4 (Inequality) storyline, which predicts an increase in inequality within economies and therefore refer to this scenario as SSP3/4.

The SSPs mainly describe macro-level storylines and scenarios of future development but provide limited detail on driving forces at spatial and micro scales, which are key determinants of income distribution and poverty. For this reason, we included an additional set of drivers in line with the SSP scenario framework (Table 1). For the macro-level, we used the standard SSP1-SSP3 GDP and population projections from the SSP scenario database (SSP Database, 2016) as input for MAGNET. To capture the spatial dynamics, we created subnational projections for all five constraint variables that we consider as main driving forces of household income distribution at the local-level. To construct the demographic (age and sex), urbanization and structural change (occupation structure) projections, we integrated a wide number of data sources, including high-resolution population data (Pezzulo et al., 2017), the Ethiopian population census (Minnesota Population Center, 2019), labor statistics (ILO, 2023) and spatially explicit demographic and urbanization SSP projections (Jones and O'Neill, 2016). The subnational projections were prepared for all 60 administrative level 2 zones in Ethiopia, spanning the period 2020–2050. Finally, we added SSP-specific assumptions on labor income changes and redistribute policies that have an effect on micro-level (i.e. household and per capita) income (see Supplementary Section 3 for more information on the construction of the subnational projections).

Table 1
Summary of scenario assumptions at different scales. τ is a flat household income tax that ensures a basic income is transferred to all persons older than 15 years. κ is a flat household income tax to simulate a universal pension for people of age 65 and above. See Supplementary Section 3 for details.

topic	element	SSP1	SSP2	SSP3/4
Macro	GDP growth	High	Medium	Low
Macro	Population growth	Relatively low	Medium	High
Spatial	Demographic change	Relatively low	Medium	High
Spatial	Urbanization	High	Medium	Low
Spatial	Structural change	Rapid	Medium	Low
Micro	Labour income trends	Neutral	Neutral	Diverging
Micro	Basic income cash transfer	Substantial (τ = 40%)	None (τ = 0%)	None (τ = 0%)
Micro	Pension cash transfer	Substantial (κ = 20%)	None (κ = 0%)	None (κ = 0%)

Validation of spatial microsimulation models

Two types of validation are commonly applied in the spatial microsimulation literature (Edwards and Tanton, 2013). The first one is internal validation, which is the comparison between simulated outcomes and the data used in the model. We calculated the two most common metrics that are used for internal validation to validate the base year simulation (see Supplementary Section 7 for details): the standardized absolute error (SAE) and the R^2. Both indicators measure how well model outcomes (i.e. the sum of weights) corresponded with the constraints (Voas and Williamson, 2001). The second type of validation is external validation, which is the comparison between simulated results with (correlated) data from other sources. We used three external validation approaches. First, we compared the simulated income distribution with the observed income distribution at the level for which the ESS4 provides representative information, such as major regions and urban–rural populations. Similarity between both distributions indicates that the our modelling approach, which combines a large number of data sources and projections, is able to reproduce the observed distributional patterns. Second, we compared our subnational results with a high-resolution map (Chi et al., 2022) of relative wealth, which can be considered as a proxy for poverty. Finally, we compared our projections with those of Rao et al. (2019), who present national-level SSP projections for the Gini index.

Climate risk assessment

The income distribution maps created by MIDS can combined with information on the location of climate extremes and wider climate hazards as part of a climate risk assessment. Climate extremes are defined as the occurrence of a value of a weather or climate variable above (or below) a threshold value near the upper (or lower) ends of the range of observed values of the variable (IPCC, 2022). Examples are heat waves, droughts, floods and tropical cyclones. Climate hazards, include both climate extremes and slow-onset climate trends, including a decrease in crop yields and an increase in water scarcity as a consequence of a changing climate.

To illustrate our modelling approach to support climate risk assessments, we combined MIDS output with heat stress projections, one of the main climate hazards in Ethiopia (Conway and Schipper, 2011). A number of indicators have been developed to measure and project heat stress (e.g. Wet-bulb globe temperature, Humidex and the heat index) (Schwingshackl et al., 2021). For this application, we selected the Heat Index (HI), which was developed by the US National Oceanic and Atmospheric Administration (NOAA) for issuing heat warnings (Steadman, 1979). This index is regularly used in studies to analyze the impact of heat stress on mortality and occupational heat exposure (Burkart et al., 2011; Opitz-Stapleton et al., 2016) and has well-defined threshold values to measure heat stress intensity. We used data from Sandstad and Schwingshackl (2022), who present HI projections for combinations of SSPs and climate (Representative Concentration Pathways, RCPs) warming scenarios, generated by a range of climate models (Supplementary Section 8). To determine the severity of heat stress, we applied a HI threshold temperature of 41°C, which corresponds with the HI classification of "very hot/danger" because of the high risk of a sunstroke, and heat exhaustion as a consequence of prolonged exposure and/or physical activity (Blazejczyk et al., 2012). We used this threshold to determine the maximum number of consecutive days with extreme heat in the year 2050. Following the IPCC definition, we considered a heatwave as a period of two or more days with hot weather (IPCC, 2022).

Several studies have pointed out that climate hazards, such as heat stress, will cause migration and internal displacement of people (Clement et al., 2021; Mueller et al., 2014). According to Amakrane

et al. (2023), this will also happen in Ethiopia. They found that around 750 thousand people are expected to leave the Adama Valley by 2050 as a result of climate risks, while an inflow of people is projected for Northern Ethiopia. Most of the displacement is expected to take place within Ethiopia. To account for climate mobility in the heat stress risk assessment, we replaced the SSP3/4 population projections, which assume no climate change, with SSP3-RCP6.0 projections (Amakrane et al., 2023) that reflect the impact of multiple climate hazards on internal migration in Africa (Supplementary Section 3) assuming a combination of SSP3 and RCP6.0 – high greenhouse gas concentration – scenarios.

Results

Fig. 2 shows the drivers for the North Gondar zone, which we use as an example to illustrate our modelling approach. North Gondar, located in the Amhara region, had a total population of over 4 million people in 2020, of which around six percent lived in rural areas. The largest share of the population were children in the age of 0–14. The majority of the labor force was categorized as low-skilled agricultural and craft, and services workers, while there were only a few clerks, professionals and technicians. Also many people were registered as not being in the labor force. Supplementary Section 6 presents the drivers for a fully urbanized area (Dire Dawa) and for a very rural zone (Borena, Guji), which, together with North Gondar, can be considered as representative for the various zones in Ethiopia.

Fig. 2 also depicts future demographic trends and structural change patterns that are in line with the SSP scenarios. In SSP1, total population growth was limited but there was a large increase in the urban population. Although agricultural and crafts, and services workers still make up the largest share of the labor force, there was strong growth in the number of high-skilled professionals and engineers. Labor income of all occupations and pensions were increasing between around 1–3% per year. In SSP3/4, population growth was much higher, resulting in a larger number of children and an increase in both the rural and urban population segments, although growth in the latter was relatively low. At the same time, the share of agricultural and crafts and services workers was growing and there was no increase in high-skilled workers. Real labor income was decreasing for low-skilled workers and slightly increasing for high-skilled workers. As expected, the trends for the SSP2 scenario, which represents a business-as-usual future, were roughly in between those of SSP1 and SSP3/4.

Fig. 3 depicts the poverty trends for North Gondar, which are determined by the combination of driving forces in Fig. 2. The average poverty rate in 2020 was 27% in 2020, most of which were children, agricultural and craft workers and people that were not in the labor force, living in rural areas. In SSP1 and SSP2 the average poverty decreased substantially to near 0% and 5%, respectively, whereas in SSP3/4 it increased to 35%, most of which were children. The increasing Gini-index in SSP2 and SSP3/4 indicates that inequality is expected to grow over time, while in SSP1 it is reduced considerably. The poverty projections for the other example zones were comparable across SSP

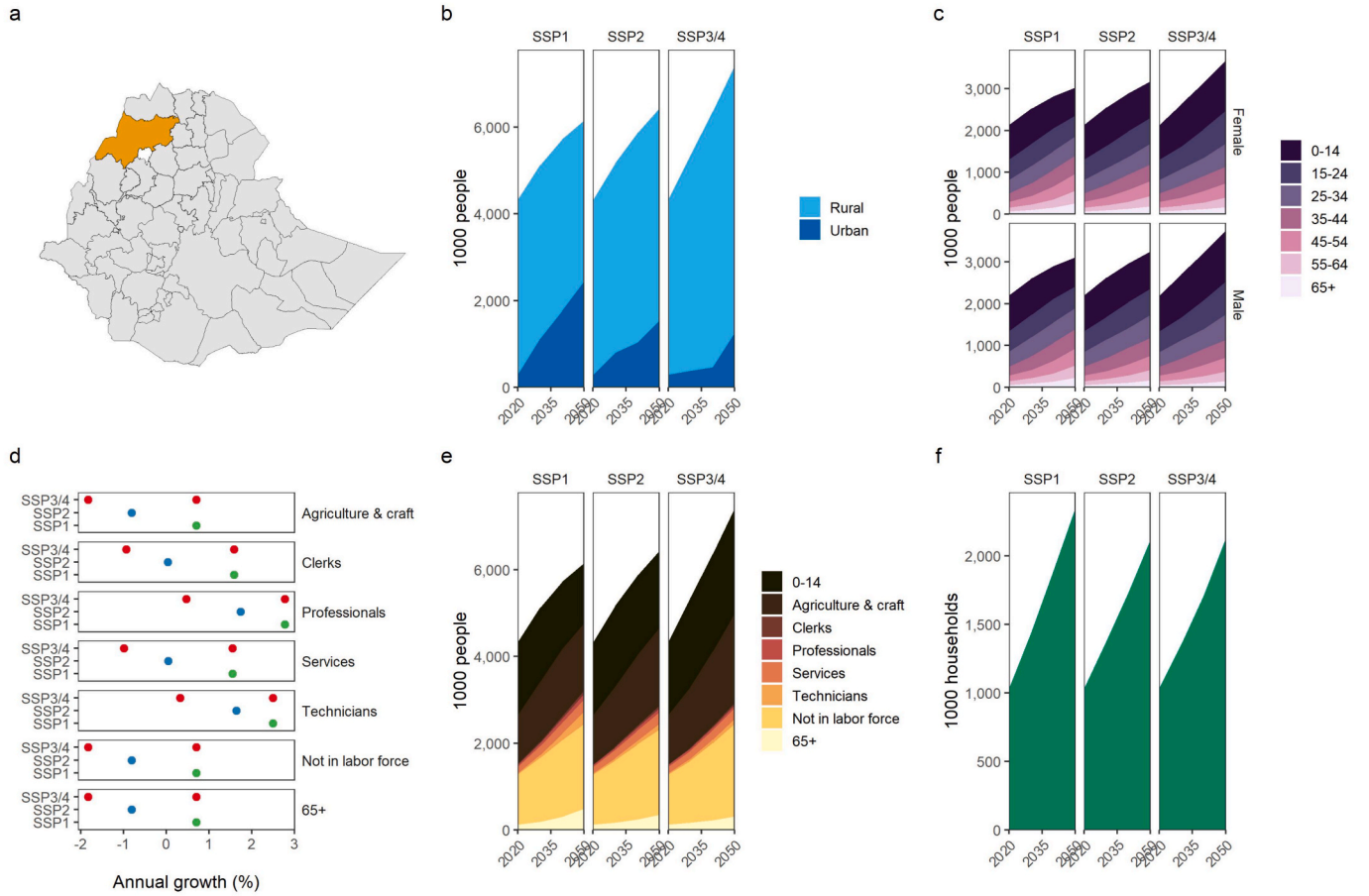

Fig. 2. SSP driver projections for North Gondar for the period 2020–2050. (a) Map of Ethiopia with location of North Gondar in yellow; (b) Urban-rural status projections, (c) Age-sex distribution projections, (d) Labor income growth by occupation class. In SSP3/4, SSP1 MAGNET labor income growth rates were applied to the upper two household income quintiles and SSP3/4 growth rates to the remaining households. For SSP1 and SSP2, the scenario-specific labor income growth rates were applied to all households, (e) Occupation class projections, (f) Number of household projections. (For interpretation of the references to colour in this figure legend, the reader is referred to the web version of this article.)

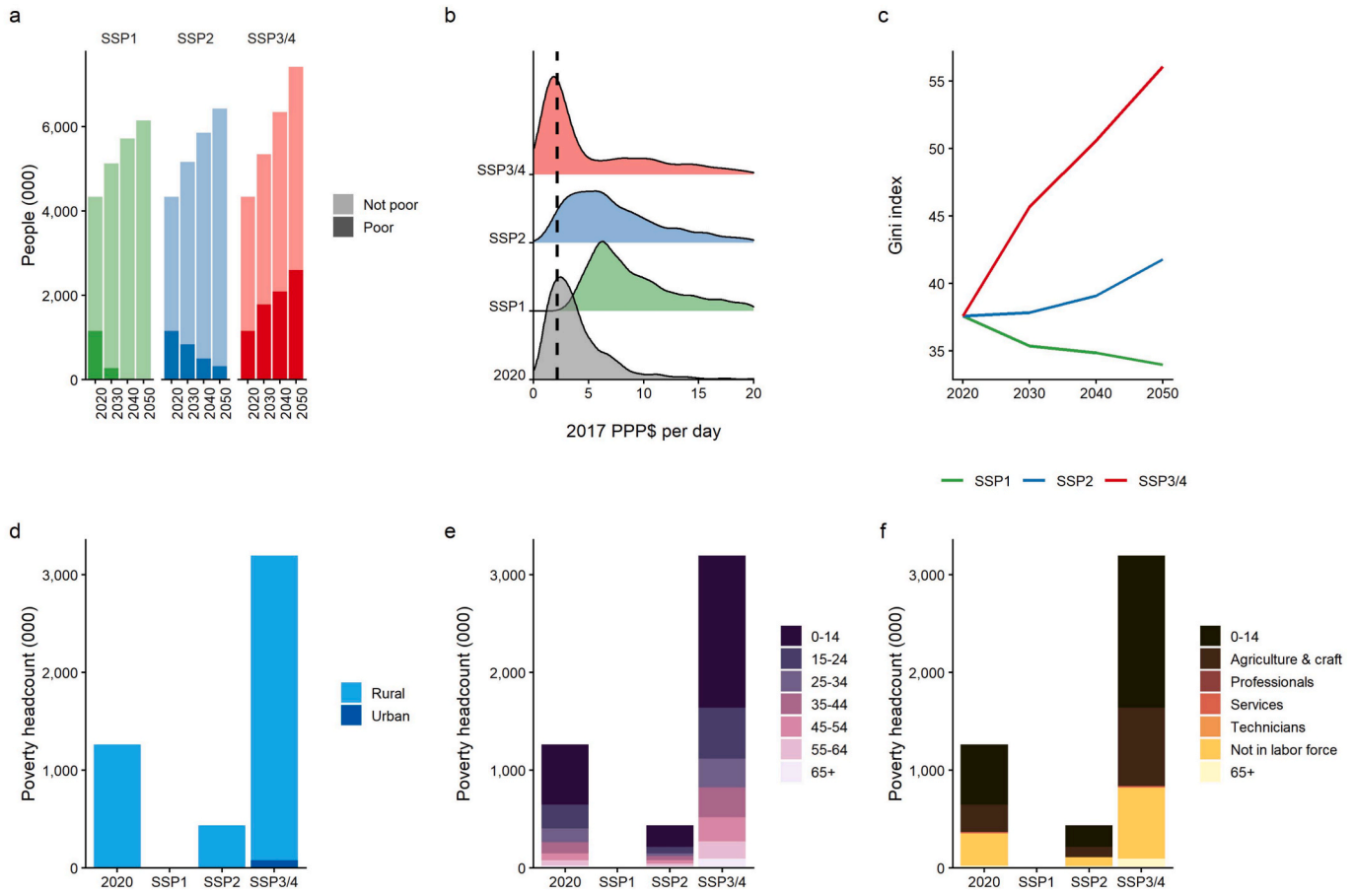

Fig. 3. Poverty outcomes for North Gondar for the year 2020 and three SSPs for the year 2050. (a) Zonal population and poverty rate, (b) Income distribution. The vertically dashed line indicates the international poverty line of $2.15 per day, (c) Gini index, (d) Poverty headcount by urban–rural status, (e) Poverty headcount by age-sex, (f) Poverty headcount by occupation class.

scenarios but differ at the more detailed level (Supplementary Section 6).

Similar to North Gondar, we calculated and projected the poverty rates across all 60 zones and for all three SSPs in Ethiopia. Fig. 4 depicts the geographical distribution of the poverty headcount rate for the three SSP scenarios as well as the national total. For the whole country, the poverty rate was 28% in 2020. In SSP1 the poverty headcount rate was projected to decrease to near zero, while in SSP2 it was around 5% by 2050. In SSP3, 34% of the households were expected to be poor in 2050. The maps show that there is variation in the poverty rate between zones. In SSP1, differences are small and poverty is below 1% in all zones. In SSP2, poverty is the lowest in the large cities (Addis Ababa, Bahir Dar, Dire Dawa and Harari) and the highest in the (mostly rural) zones in the Somali region, which were already characterized by high poverty levels in 2020. In SSP3/4, poverty is more profound and widespread, with the highest poverty rates in Gambela, Affar, Oromia and Somali zones, while in the large cities the number of poor people only slightly increased.

Validation results

Fig. 5 summarizes the results of the internal and external validation exercises. For all scenarios, the SAE for 80% of the areas is below the 15% threshold that is often used in the literature (Fig. 5a). The model performance for SSP1 in the year 2050 is just above the minimum threshold value, while the projections for the other SSPs show lower SAE values. This can be explained by the fact that changes in the constraints are more extreme in SSP1 than for other SSPs. This holds particularly for the occupation constraints (e.g. growth in high-skilled occupations), because of deeper structural economic transformation and more urbanization in SSP1. Because the sample contained only a limited number of high-skilled urban households, adjusting the weights was challenging and the SAE therefore tends to be larger for these constraint classes. However, although the SAE is relatively large, the absolute size of the constraint classes is small (i.e. relatively low number of people with a high-skilled occupation) and the overall model performance remains strong, as indicated by the high R^2 between simulated and observed constraints (Supplementary Section 6).

Fig. 5b shows a good match between the simulated poverty headcount ratio and the relative wealth index (R^2 of 0.52). Both sources produce the lowest poverty rates for large city areas (Addis Ababa, Bahir Dar, Dire Dawa and Harari, indicated by the four observations on the left) and higher poverty rates for rural zones. The resemblance between the small area estimates from MIDS and the relative wealth index is striking as the poverty estimates were produced using two different approaches (spatial microsimulation versus machine learning) and used different sources (ESS4 versus Dietary Health Surveys).

Fig. 5c and d compare the distribution in ESS4 and simulated per capita income values for the year 2020 at the region-level and for urban and rural populations, respectively. All figures are based on the same base year household income data from the survey but use different weights (i.e. observed versus simulated). Both the median and the shape of simulated distributions resemble the log-normal distribution observed in the ESS4 data. Only in the case of SNNP and urban areas, the microsimulation seems to slightly underestimate the median value. The simulated distributions are less smooth than the survey distributions because they are based on a much larger number of observations,

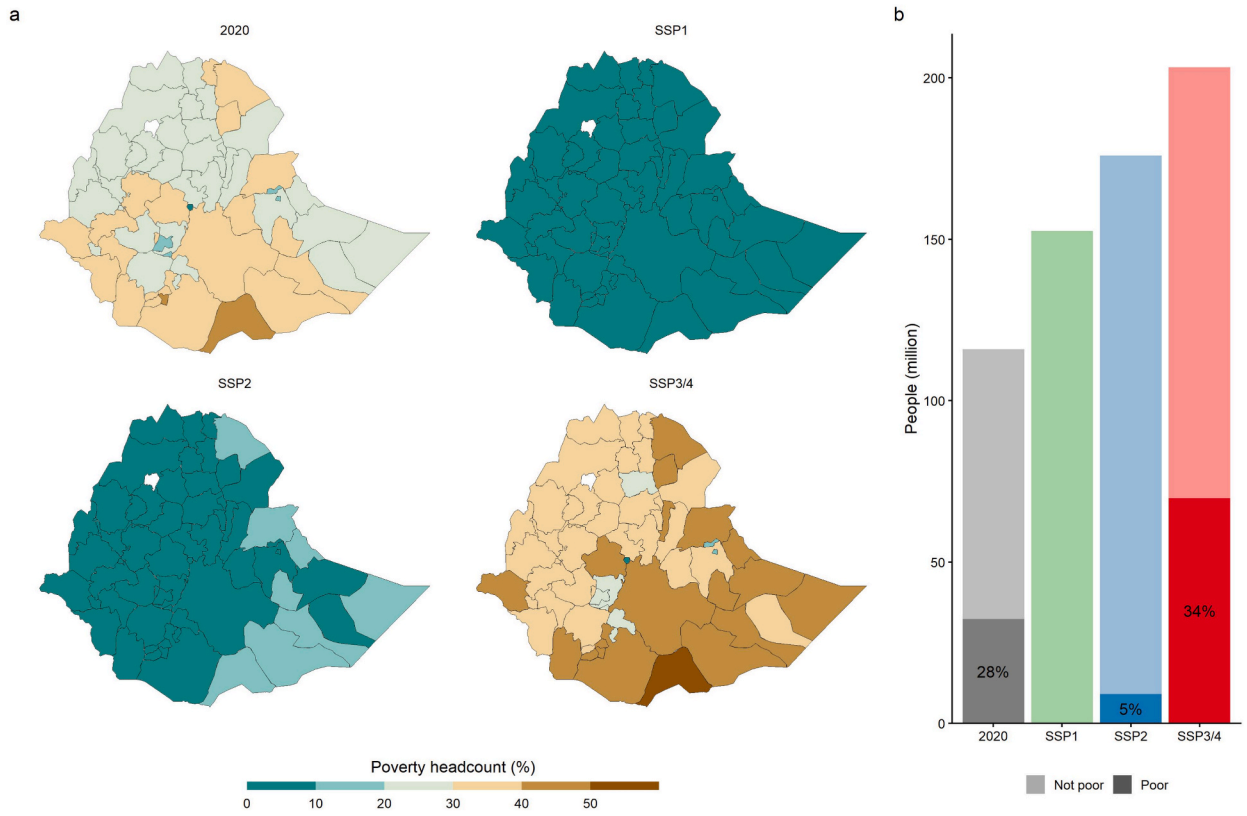

Fig. 4. (a) Geographical distribution of the poverty headcount rate in Ethiopia for 2020 and three SSPs for 2050, (b) National-level poverty rate for 2020 and three SSPs.

namely the full household survey sample reweighted for each zone and urban/rural area.

Finally, we compared our national-level Gini-index projections with those of Rao et al. (2019), who used an econometric approach to project inequality for each of the SSPs. Our results are very similar for SSP1 but differ for the other two scenarios (Supplementary Fig. 8). We predicted an increase in the Gini index for these scenarios, whereas Rao et al. (2019), projected a slight decrease in equality in SSP2 and only a small increase in SSP3 and SSP4, which seem to contradict with the storylines of these SSPs. The approach of Rao et al. (2019) is based on a cross-country econometric model that assumes changes in the Gini-index are primarily driven by macro-level factors, such as education, trade and technology. As a result, it may not adequately capture the impact of sectoral and micro-drivers of income distribution. In contrast, the MIDS model explicitly simulates how changes in income distribution and poverty are driven by shifts in the composition of the population (e.g. urbanization and structural economic transformation) and changes in labor income. Consequently, the model produces inequality projections that are more consistent with the SSP storylines.

Risk assessment of future heat stress

Similar to the poverty projections, areas with extreme heat are not evenly distributed over the different zones in Ethiopia in 2050. Extreme temperatures are most likely to be observed at the borders of the country, while temperatures are lower in the center (Supplementary Section 8). Fig. 6a combines temperature and poverty information to reveal the zones, which are both characterized by a high probability of heat stress and a large vulnerable population as measured by the number of poor people. North Gondar can be regarded as a hotspot of high heat stress risk in both scenarios. Eastern Tigray and Zone 2, in the North of Ethiopia stand out as zones with a very large number of days with extreme HI and a high number of poor people in SSP3/4-RCP7.0. We found that almost 1.4 million poor people, equal to around 1% of the total projected population in 2050, will be exposed to heat waves in SSP2-RCP4.5. With 9.4 million or around 5% of the total population, this number is much higher in SSP3/4-RCP7.0, which is characterized by higher population growth, higher poverty and higher climate impact (Fig. 6b). The majority of the vulnerable poor live in rural areas and primarily include children and agricultural and craft workers.

To analyze the impact of accounting for climate mobility on climate vulnerability, it is useful to compare the results of the SSP3/4-RCP7.0 scenario with those of the baseline SSP3/4 scenario, which assumes no climate change (Supplementary Fig. 11). At the aggregate level, we found that the the total number of poor people at risk of extreme heat is almost identical in both scenarios (approximately 9.4 million people). However, substantial differences emerge in the spatial distribution of people vulnerable to heat stress. In the SSP3-RCP7.0 scenario, the number of poor people is up to 40% higher in the northwestern Ethiopia and around 25% lower in the southern and central parts of the country as a consequence of climate-induced migration in comparison to the SSP3/4 scenario. North-Western Tigray is one of the zones with the highest number of poor people exposed to substantial heat stress (dark green areas) in the SSP3-RCP7.0 scenario, whereas this is not the case in the SSP3/4 scenario. In several other zones (e.g. Metekel, Shinile and West Welega), the projected number of poor people exposed to heat waves differs considerably between the two scenarios.

Discussion

In this paper, we proposed an innovative modelling approach to simulate changes in income distribution and poverty in space and over time. Despite our efforts to build a robust and empirically sound model it is important to highlight several limitations that should be taken in mind when interpreting the results.

First, poverty is a complex phenomenon that is determined by the

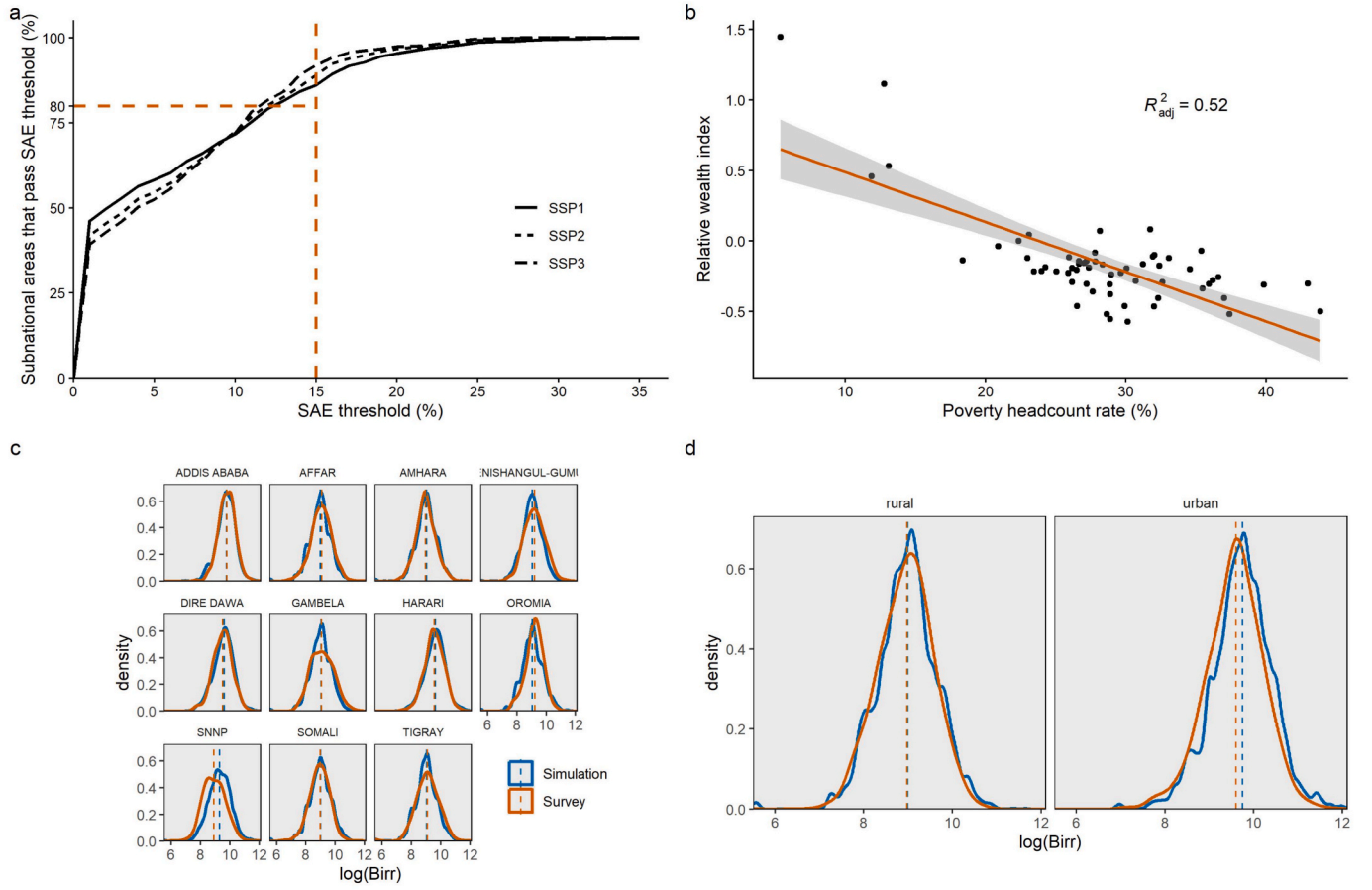

Fig. 5. Model validation results. (a) Percentage of subnational areas that pass the SAE threshold per scenario (pooled years and constraints). Vertical dashed lines show the minimum SAE threshold values that are used in the literature (Supplementary Section 7). Values are computed individually for each combination of zone, year, scenario and constraint class. The orange dashed lines indicate a SAE threshold of less than 15% in at least 80% of the areas, (b) Regression of the relative wealth index (Chi et al., 2022) on the simulated poverty headcount ratio for 2020 at the zonal-level. Comparison between weighted kernel distribution for log per capita income based on the ESS4 data and (c) simulated results at the region-level, and (d) simulated results for urban and rural populations for 2020. (For interpretation of the references to colour in this figure legend, the reader is referred to the web version of this article.)

interaction of a large number of drivers. It is important to emphasize that the MIDS model is a simplification of reality, which does not aim to predict future poverty. Instead, its objective is to incorporate the main drivers of income distribution to assess the plausible future 'bandwidth' of poverty under different scenarios that describe the change in these drivers. One of the driving forces of income distribution that is frequently highlighted in the literature, but not explicitly taken into account by MIDS, is educational attainment (Rao et al., 2019). Ideally, we would have added education as an additional constraint in the spatial microsimulation to grasp its effect on income distribution and poverty. Unfortunately, and in contrast to the other drivers, there are no data sources that provide detailed subnational information on the breakdown by education level, which are compatible with the SSP education projections. However, we believe that this is not a major problem as several of the drivers that are implemented by MIDS, in particular occupational structure, are highly correlated with educational attainment (Gibbons et al., 2005) and therefore account for the impact of human capital on income. At present, MIDS does not account for the impact of highly local determinants of poverty, such as access to roads, soil quality and land cover (Chi et al., 2022; Okwi et al., 2007). In theory, it would be technically feasible to add these variables as additional constraints in the spatial microsimulation if (a) the household survey would provide this information for each household and (b) subnational information and projections would be available from secondary sources (Birkin and Clarke, 2012). In practice, these data are almost never available.

Second, and somewhat related to the previous point, the model only partially accounts for spatial drivers of income and poverty. We used national level projections for labor income change from a global CGE model to project subnational household income. In reality, labor income changes will not be the same between regions due to differences in local market conditions, household characteristics and urbanization level. An alternative approach would be to use output from national-level CGE models, which often include major administrative units and several representative household groups (Dorosh and Thurlow, 2014). The disadvantage of using a single-country CGE is that such models do not take into account international trade dependencies, which are shown to be an important driver of poverty and inequality (Anderson, 2020), especially when countries go through a process of structural transformation (Uy et al., 2013).

Third, it is important to note that the current model setup primarily captures the impact of socio-economic drivers (e.g. technical change, structural transformation and urbanization) on future income distribution and poverty. MIDS does not account for the impact of climate change and climate shocks on future household income, for example because of the negative impact of droughts on crop yields, losses in production due to floods or reduced labor capacity because of extreme heat. Therefore, the poverty projections that result from our modelling framework should be regarded as no climate change scenarios and, in particular for the more extreme SSP3/4-RCP7.0 scenario, will likely underestimate post-hazard household income. Nonetheless, several studies point out that the impact of socio-economic drivers, such as demographic change and economic development, which determine

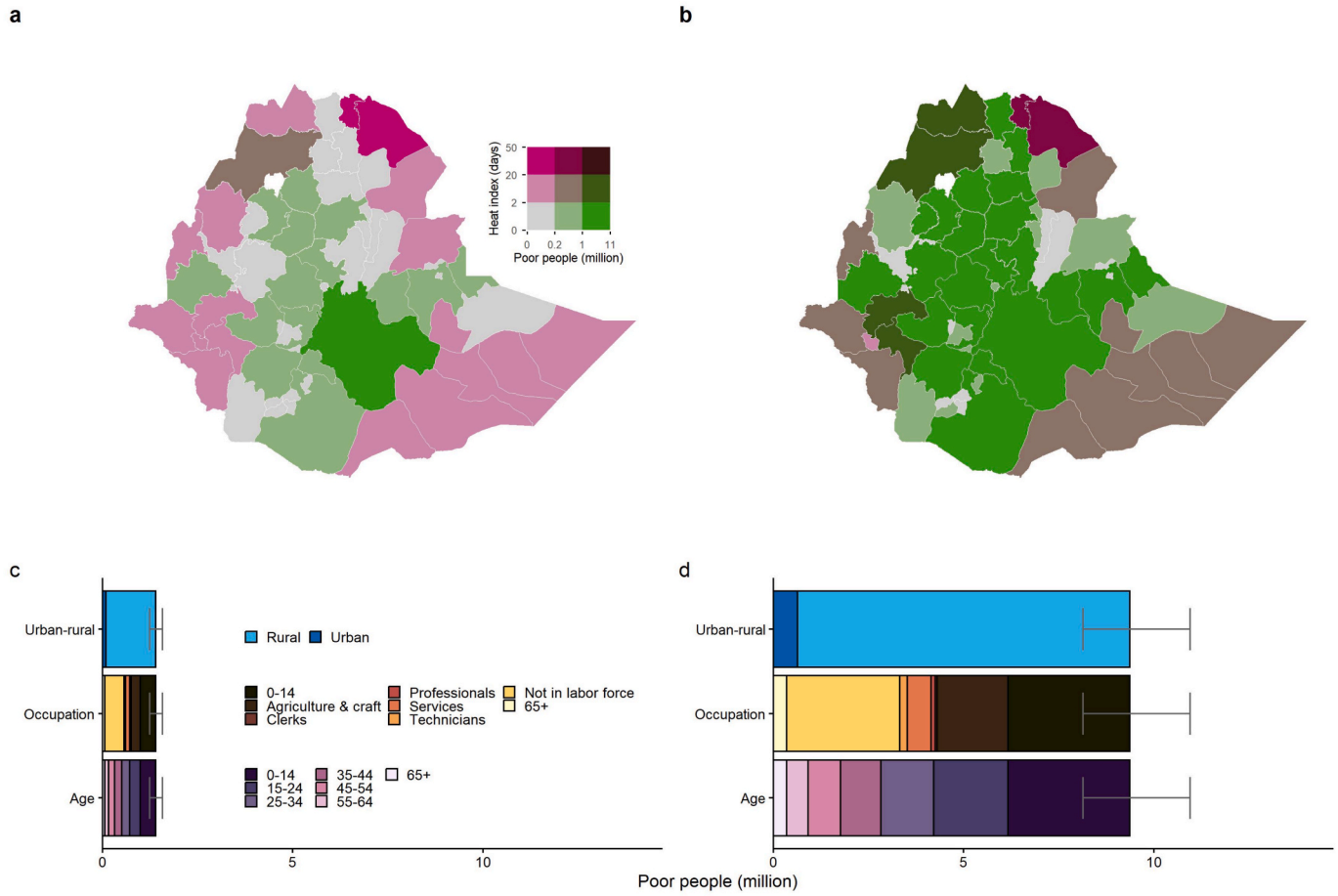

Fig. 6. Overlay of SSP poverty headcount and RCP HI maps in 2050 for (a) SSP2-RCP4.5 and (b) SSP3/4-RCP7.0 scenarios. Number of poor people exposed to a heat wave in 2050 by urban-rural status, occupation class and age structure for (c) SSP2-RCP4.5 and (d) SSP3/4-RCP7.0 scenarios. The error bars indicate climate model uncertainty. Results for SSP1 are not depicted because the number of poor people is close to zero in this scenario. Population projections for SSP3/4-RCP7.0 are taken from Amakrane et al. (2023) and account for the impact of climate change on internal migrations under an RCP6.0 climate scenario (Supplementary Section 3). Heat stress is measured as the number of two or more consecutive days with a HI of above 41°C.

vulnerability and exposure, have a larger impact than hazards, such as heat stress, on climate risk (Landreau et al., 2021; Rohat et al., 2019). Hence, we believe that the main value of our modelling approach is to capture the impact of socio-economic change on future poverty and to use this information to better understand the exposure and vulnerability of the poor to climate hazards.

Fourth, we used a top-down approach to link the macro CGE output with the spatial microsimulation approach, which does not take into account any feedback loops between the two levels of modeling. For example, we did not account for the impact of micro-level changes in income and consumption on macro-level prices, wages and labor supply. An improvement would be to implement a top-down bottom-up method that involves an iterative process in which both models exchange information till they converge to a joint solution (Colombo, 2010; Peichl, 2016). However, these advanced methods are also not free from theoretical and conceptual difficulties, which makes their implementation complex. Moreover, a comparison indicated that the top-down method can be considered as a satisfactory approximation of more advanced two-way interaction approaches (Bourguignon and Savard, 2008).

Finally, the MIDS model requires a relatively large amount of detailed and spatially explicit information, drawn from a range of sources, including global datasets, high-resolution maps, the population census and a large household survey. This means that the outputs of the model are invariably influenced by the availability, quality and consistency of the input data. For instance, the creation of subnational demographic, occupation and urbanization projections involved the downscaling and harmonization of several spatial and national datasets, which could have introduced a bias. Ideally, subnational projections of drivers should be created using granular spatial statistics (Jiang et al., 2020), which are often not available for low-income countries like Ethiopia. Similarly, we used a relatively small household survey, which mag have resulted in a loss of spatial diversity as extreme values (e.g. regions with a large share of wealthy households) might not have been fully captured (Birkin and Clarke, 2012). We would have liked to use the Ethiopian Household Income and Consumption Expenditure Survey (HICES), the official source to estimate national poverty statistics, which contains a representative sample for a much larger number of subnational units. Unfortunately this data set was not publicly available. Lastly, for the most extreme scenario (SSP3) in the heat stress risk assessment, we incorporated climate projections that were adjusted for climate mobility. However, these projections were based on a different climate warming scenario (RCP6.0) than the one used for the heat stress projections (RCP7.0), which could have introduced inconsistencies in the results.

In the future, we aim to deepen and expand our research in a number of directions. First, we would like to apply the model to multiple countries to assess climate risk and poverty dynamics at scale in regions that are regarded as the most vulnerable to climate change, in particular Africa and Asia. The main bottleneck in rolling out the model is the availability of household income and expenditure surveys, which are often outdated or not accessible. A positive development in this regard are initiatives such as the World Bank Living Standards Measurement

Study – Integrated Surveys on Agriculture (LSMS-ISA) program that facilitates open access to these datasets (World Bank, 2026).

Second, we aim to enhance the modelling framework to simulate the impact of climate hazards on subnational income distribution and poverty. One interesting option would be to extend our CGE model so that it factors in the impact of climate change on labor capacity and agricultural productivity, which would, in turn, affect wages and prices (De Lima et al., 2021). Studies show that especially heat stress negatively affects the productivity of farmers and farm workers, which are among the most vulnerable to climate change (Dasgupta et al., 2024). Another option would be to explore ways to directly incorporate the impact of climate change on individual household income in the MIDS model, for example by using econometric approaches to quantify the change in temperature on poverty (Dang et al., 2026) and by estimating and adding a measure for household resilience capacity, which mitigates the impact of climate extremes (Upton et al., 2022).

Finally, we provided a simple heat stress risk assessment to illustrate how the results of our modelling approach can be used. It would be interesting to expand this analysis and quantify the number and profile of poor people that are exposed to multiple climate hazards, such as floods, droughts and wildfires (Byers et al., 2018; Piontek et al., 2014). Overlaying spatial information on climate extremes and poverty maps, will also make it possible to better quantify the effect of climate shocks on poverty by taking into account local impacts, which is not possible with the existing aggregate approaches (Hallegatte and Rozenberg, 2017; Rao et al., 2017).

The results of the heat stress risk assessment indicate that a large number of poor people in Ethiopia will be exposed to extreme heat in the future, especially under the more extreme SSP3/4-RCP7.0 scenario. This highlights the need for policies aimed at reducing the vulnerability of poor people to heat stress. Our assessment indicates that in particular in northern Ethiopia, a large number of poor people are expected to be exposed to future heat stress, which calls for targeted interventions in these areas, such as the development and implementation of heat action plans, the improvement of housing conditions the provision of cooling centers and the establishment of early warning systems. The most recent Ethiopian Nationally Determined Contributions (NDC) (Federal Democratic Republic of Ethiopia, 2021), which outline national strategies for climate adaptation, does not identify heat stress as a priority, nor does it provide detailed information on regional risks or specific adaptation measures. The results of this study could therefore help to improve and further develop the next iteration of the Ethiopian NDC.

Conclusions

In this paper we present the Microsimulation of Income DynamicS (MIDS) model, which combines dynamic spatial microsimulation with inputs from a CGE model to provide future trends in income distribution and poverty at the subnational level under different socio-economic pathways (SSP), with an application to Ethiopia. To simulate subnational and household-level impacts, we prepared spatial projections of key driving forces and introduced additional assumptions on micro-level drivers of income distribution (i.e. redistributional taxes and subsidies) that are consistent with the SSP storylines.

The main outputs of MIDS are poverty maps that illustrate how income distribution evolves over time and space as a result of the combined effect of global, national and spatial drivers. These outputs can be used to better evaluate the exposure of the poor to climate extremes. This was demonstrated by combining the poverty maps with spatial information on future heat stress, which showed that under the most extreme climate and socio-economic scenario 9.4 million poor people equal to 5% of the population will be exposed to heat waves in 2050.

Our results further indicate that climate mobility significantly affects the spatial distribution of people vulnerable to heat stress, highlighting the importance of incorporating climate-induced migration in subnational climate risk assessments. The MIDS modelling framework helps to identify regions with the highest concentration of vulnerable people at risk of heat stress, which will be useful to support the design of targeted climate adaptation strategies and action plans.

CRediT authorship contribution statement

Michiel van Dijk: Writing – review & editing, Writing – original draft, Software, Investigation, Formal analysis, Data curation, Conceptualization. **Marijke Kuiper:** Writing – review & editing, Investigation. **Thijs de Lange:** Writing – review & editing, Investigation. **Jason F.L. Koopman:** Writing – review & editing, Investigation. **Willem-Jan van Zeist:** Writing – review & editing, Investigation.

Declaration of competing interest

The authors declare that they have no known competing financial interests or personal relationships that could have appeared to influence the work reported in this paper.

Acknowledgements

Funding: Contributions of M.v.D and J.F.L.K were supported by the Dutch Ministry of Agriculture, Nature and Food Security funded Food and Water Security programme [KB35-103-002]. This publication is part of the project Senior Expert Foresight for Food System Transformation (F4FST) with file number INT.1723.24.005 of the Senior Expert Programme (SEP) II which is (partly) financed by the Dutch Research Council (NWO) under the grant https://doi.org/10.61686/VKQZT84670.

Declaration of generative AI and AI-assisted technologies in the manuscript preparation process.

During the preparation of this work the author(s) used ChatGPT for language editing and improving clarity in the introduction, discussion and conclusions sections. After using this tool/service, the author(s) reviewed and edited the content as needed and take(s) full responsibility for the content of the published article.

Appendix A. Supplementary data

Supplementary data to this article can be found online at https://doi.org/10.1016/j.cliser.2026.100668.

Data availability

The Ethiopian household survey is available from World Bank Living Standards Measurement Study - Integrated Surveys on Agriculture (LSMS-ISA), https://www.worldbank.org/en/programs/lsms/initiatives/lsms-ISA. The 2007 Ethiopian census is available from IPUMS international: https://international.ipums.org/international/. Macro-level SSP projections can be downloaded from the SSP scenario database: https://tntcat.iiasa.ac.at/SspDb. Subnational population projections can be downloaded from NASA Earth Data: https://www.earthdata.nasa.gov/data/catalog/sedac-ciesin-sedac-pd-dpopssp-1.0 (baseline) and https://doi.org/10.7927/5tv3-ff20 (climate mobility). Subnational age-sex maps are available from WorldPop: https://www.worldpop.org/. National population and urbanization projections are available from UNDESA: https://population.un.org/wup/. National labor projections are available from the ILO: https://ilostat.ilo.org/. Heat stress projections are available from the Climate Data Store: https://doi.org/https://doi.org/10.24381/cds.776e08bd.

References

Acemoglu, D., Johnson, S., Robinson, J.A., 2002. Reversal of fortune: geography and institutions in the making of the Modern World Income distribution. Q. J. Econ. 117 (4), 1231–1294. https://doi.org/10.1162/003355302320935025.

Adshead, D., Paszkowski, A., Gall, S.S., Peard, A.M., Adnan, M.S.G., Verschuur, J., Hall, J.W., 2024. Climate threats to coastal infrastructure and sustainable development outcomes. Nat. Clim. Chang. 14 (4), 344–352. https://doi.org/10.1038/s41558-024-01950-2.

Ahmed, A., Bussolo, M., Cruz, M., Go, D.S., Osorio-Rodarte, I., 2020. Global Inequality in a more educated world. J. Econ. Inequal. 18 (4), 585–616. https://doi.org/10.1007/s10888-020-09440-z.

Amakrane, K., Rosengaertner, S., Simpson, N., de Sherbinin, A., Linekar, J., Horwood, C., Forin, R., 2023. African shifts: the africa climate mobility report, addressing climate-forced migration & displacement. Africa Climate Mobility Initiative; Global Centre for Climate Mobility, New York.

Andersen, R., 2008. Modern Methods For Robust Regression. SAGE Publications Inc, Thousand Oaks.

Anderson, E., 2020. The impact of trade liberalisation on poverty and inequality: evidence from CGE models. J. Policy Model 42 (6), 1208–1227. https://doi.org/10.1016/J.JPOLMOD.2020.05.006.

Berhanu, A.A., Ayele, Z.B., Dagnew, D.C., Fenta, A.B., Kassie, K.E., 2024. Smallholder farmers' coping strategies to climate change and variability: evidence from Ethiopia. Clim. Serv. 35, 100509. https://doi.org/10.1016/j.cliser.2024.100509.

de Beyer, J., Knight, J.B., 1989. The role of occupation in the determination of wages. Oxf. Econ. Pap. 41 (3), 595–618.

Birkin, M., Clarke, G., 2012. The enhancement of spatial microsimulation models using geodemographics. Ann. Reg. Sci. 49 (2), 515–532. https://doi.org/10.1007/S00168-011-0472-2/METRICS.

Blazejczyk, K., Epstein, Y., Jendritzky, G., Staiger, H., Tinz, B., 2012. Comparison of UTCI to selected thermal indices. Int. J. Biometeorol. 56 (3), 515–535. https://doi.org/10.1007/S00484-011-0453-2/FIGURES/12.

Bourguignon, F., Bussolo, M., 2013. Chapter 21 – income distribution in computable general equilibrium modelling. In: Handbook of Computable General Equilibrium Modeling, pp. 1383–1437. https://doi.org/10.1016/B978-0-444-59568-3.00021-3.

Bourguignon, F., Savard, L., 2008. Distributional effects of trade reform: an integrated macro-micro model applied to the Philippines. In: Bourguignon, F., Bussolo, M., Pereira da Silva, L.A. (Eds.), The Impact of Macroeconomic Policies on Poverty and Income Distribution. Palgrave Macmillan, Houndsmills, pp. 177–211.

Burkart, K., Schneider, A., Breitner, S., Khan, M.H., Krämer, A., Endlicher, W., 2011. The effect of atmospheric thermal conditions and urban thermal pollution on all-cause and cardiovascular mortality in Bangladesh. Environ. Pollut. 159 (8–9), 2035–2043. https://doi.org/10.1016/J.ENVPOL.2011.02.005.

Burke, M., Hsiang, S.M., Miguel, E., 2015. Global non-linear effect of temperature on economic production. Nature 527 (7577), 235–239. https://doi.org/10.1038/nature15725.

Bussolo, M., De Hoyos, R.E., Medvedev, D., 2010a. Economic growth and income distribution: linking macro- economic models with household survey data at the global level. Int. J. Microsimul. 3 (1), 92–103.

Bussolo, M., de Hoyos, R.E., Medvedev, D., van der Mensbrugghe, D., 2010b. Global growth and distribution: are China and India reshaping the world. In: Santos-Paulino, A.O., Wan, G. (Eds.), Southern Engines of Global Growth. Oxford University Press, pp. 77–113.

Byers, E., Gidden, M., Leclere, D., Balkovic, J., Burek, P., Ebi, K., Riahi, K., 2018. Global exposure and vulnerability to multi-sector development and climate change hotspots. Environ. Res. Lett. 13 (5), 055012. https://doi.org/10.1088/1748-9326/aabf45.

Central Statistics Agency of Ethiopia. (2020). *Socioeconomic Survey 2018-2019*. https://doi.org/. https://doi.org/10.48529/3GMA-7G23.

Chi, G., Fang, H., Chatterjee, S., Blumenstock, J.E., 2022. Microestimates of wealth for all low- and middle-income countries. Proc. Natl. Acad. Sci. 119 (3), e2113658119. https://doi.org/10.1073/pnas.2113658119.

Clement, V., Rigaud, K.K., De Sherbinin, A., Jones, B., Adamo, S., Schewe, J., Shabahat, E., 2021. Groundswell Part 2: acting on Internal Climate Migration. World Bank, Washington DC.

Colombo, G., 2010. Linking CGE and microsimulation models: a comparison of different approaches. Retrieved from Int. J. Microsimul. 3 (1), 72–91. http://www.microsimulation.org/IJM/V3{_}1/IJM{_}20.pdf.

Conway, D., Schipper, E.L.F., 2011. Adaptation to climate change in Africa: challenges and opportunities identified from Ethiopia. Glob. Environ. Chang. 21 (1), 227–237. https://doi.org/10.1016/J.GLOENVCHA.2010.07.013.

Dang, H.-A.-H., Hallegatte, S., Nguyen, M.C., Trinh, T.-A., 2026. Impacts of global warming on subnational poverty and inequality. Nat. Clim. Chang. 16 (2), 207–213. https://doi.org/10.1038/s41558-025-02516-6.

Dasgupta, S., Robinson, E.J.Z., Shayegh, S., Bosello, F., Park, R.J., Gosling, S.N., 2024. Heat stress and the labour force. Nat. Rev. Earth Environ. 5 (12), 859–872. https://doi.org/10.1038/s43017-024-00606-1.

De Lima, C.Z., Buzan, J.R., Moore, F.C., Baldos, U.L.C., Huber, M., Hertel, T.W., 2021. Heat stress on agricultural workers exacerbates crop impacts of climate change. Environ. Res. Lett. 16 (4), 44020. https://doi.org/10.1088/1748-9326/abeb9f.

Diffenbaugh, N.S., Burke, M., 2019. Global warming has increased global economic inequality. PNAS 116 (20), 9808–9813. https://doi.org/10.1073/PNAS.1816020116/SUPPL_FILE/PNAS.1816020116.SAPP.PDF.

Dollar, D., Kleineberg, T., Kraay, A., 2016. Growth still is good for the poor. Eur. Econ. Rev. 81, 68–85. https://doi.org/10.1016/j.euroecorev.2015.05.008.

Dorosh, P., Thurlow, J., 2014. Can cities or towns drive African development? Economywide analysis for Ethiopia and Uganda. World Dev. 63, 113–123. https://doi.org/10.1016/J.WORLDDEV.2013.10.014.

Duernecker, G., Herrendorf, B., 2022. Structural transformation of occupation employment. Economica 89 (356), 789–814. https://doi.org/10.1111/ecca.12435.

Edwards, K.L., Tanton, R., 2013. Validation of spatial microsimulation models. In: Tanton, R., Edwards, K.L. (Eds.), Spatial microsimulation: A reference guide for users, pp. 249–258 https://doi.org/10.1007/978-94-007-4623-7_15.

Federal Democratic Republic of Ethiopia. (2021). *Updated Nationally Determined Contribution*.

Gibbons, R., Katz, L.F., Lemieux, T., Parent, D., 2005. Comparative advantage, learning, and sectoral wage determination. J. Labor Econ. 23 (4), 681–724. https://doi.org/10.1086/491606.

Hallegatte, S., Bangalore, M., Bonzanigo, L., Fay, M., Kane, T., Narloch, U., Rozenberg, J., 2016. Shock Waves: Managing the Impacts of climate Change on poverty. World Bank, Washington DC.

Hallegatte, S., & Rozenberg, J. (2017). *Climate change through a poverty lens*. https://doi.org/10.1038/nclimate3253.

Harding, A., Vidyattama, Y., Tanton, R., Harding, A., Vidyattama, Y., Tanton, Á.R., Tanton, R., 2011. Demographic change and the needs-based planning of government services : projecting small area populations using spatial microsimulation. J. Pop Res. 28, 203–224. https://doi.org/10.1007/s12546-011-9061-6.

Haughton, J., Khandker, S., 2009. Measures of poverty. Handbook of poverty and inequality. World Bank, Washington, DC.

Hsiang, S., Kopp, R., Jina, A., Rising, J., Delgado, M., Mohan, S., Houser, T., 2017. Estimating economic damage from climate change in the United States. Science 356 (6345), 1362–1369. https://doi.org/10.1126/science.aal4369.

ILO. (2023). *ILOSTAT*. Retrieved from https://ilostat.ilo.org/.

IPCC, 2022. Climate Change 2022: Impacts, Adaptation and Vulnerability. Contribution of Working Group II to the Sixth Assessment Report of the Intergovernmental Panel on climate Change. Cambridge University Press, Cambridge.

Jafino, B. A., Walsh, B., Rozenberg, J., & Hallegatte, S. (2020). *Revised Estimates of the Impact of Climate Change on Extreme Poverty by 2030*. Retrieved from http://www.worldbank.org/prwp.

Jiang, L., O'Neill, B.C., Zoraghein, H., Dahlke, S., O'Neill, B.C., Zoraghein, H., Dahlke, S., 2020. Population scenarios for U.S. states consistent with shared socioeconomic pathways. Environ. Res. Lett. 15 (9), 94097. https://doi.org/10.1088/1748-9326/aba5b1.

Jones, B., O'Neill, B.C., 2016. Spatially explicit global population scenarios consistent with the Shared Socioeconomic Pathways. Environ. Res. Lett. 11 (8), 084003. https://doi.org/10.1088/1748-9326/11/8/084003.

Kirezci, E., Young, I.R., Ranasinghe, R., Muis, S., Nicholls, R.J., Lincke, D., Hinkel, J., 2020. Projections of global-scale extreme sea levels and resulting episodic coastal flooding over the 21st Century. Sci. Rep. 10 (1), 1–12. https://doi.org/10.1038/S41598-020-67736-6.

Laborde Debucquet, D., Martin, W., 2018. Implications of the global growth slowdown for rural poverty. Agricul. Econ. 49 (3), 325–338. https://doi.org/10.1111/agec.12419.

Landreau, A., Juhola, S., Jurgilevich, A., Räsänen, A., 2021. Combining socio-economic and climate projections to assess heat risk. Climatic Change 167 (1–2), 12. https://doi.org/10.1007/s10584-021-03148-3.

Lange, S., Volkholz, J., Geiger, T., Zhao, F., Vega, I., Veldkamp, T., Frieler, K., 2020. Projecting exposure to extreme climate impact events across six event categories and three spatial scales. Earth's Future 8 (12). https://doi.org/10.1029/2020EF001616.

Leclère, D., Obersteiner, M., Barrett, M., Butchart, S.H.M., Chaudhary, A., De Palma, A., Young, L., 2020. Bending the curve of terrestrial biodiversity needs an integrated strategy. Nature 585 (7826), 551–556. https://doi.org/10.1038/s41586-020-2705-y.

Liu, K., Wang, R., Schrijver, I., Hoekstra, R., 2024. Can we project well-being? Towards integral well-being projections in climate models and beyond. Human. Soc. Sci. Commun. 11 (1), 457. https://doi.org/10.1057/s41599-024-02941-6.

Lovelace, R., Dumont, M., 2016. Spatial Microsimulation with R. Hall/CRC, Chapman.

Mahler, D. G., Yonzan, N., & Lakner, C. (2022). *The Impact of COVID-19 on Global Inequality and Poverty*. Retrieved from http://www.worldbank.org/prwp.

Marzi, S., Poljanšek, K., Papadimitriou, E., Dalla Valle, D., Salvi, A., Corbane, C., 2025. Assessing future risk of humanitarian crises using projections of climate-related hazards, population, conflict and other socioeconomic variables within the INFORM framework. Big Earth Data 9 (4), 676–713. https://doi.org/10.1080/20964471.2025.2535852.

Merkle, M., Dellaccio, O., Dunford, R., Harmáčková, Z.V., Harrison, P.A., Mercure, J.-F., Rounsevell, M., 2023. Creating quantitative scenario projections for the UK shared socioeconomic pathways. Climate Risk Manage. 40, 100506. https://doi.org/10.1016/j.crm.2023.100506.

Mideksa, T.K., 2010. Economic and distributional impacts of climate change: the case of Ethiopia. Global Environ. Change 20 (2), 278–286. https://doi.org/10.1016/J.GLOENVCHA.2009.11.007.

Minnesota Population Center. (2019). *Integrated Public Use Microdata Series, International: Version 7.2*. https://doi.org/https://doi.org/10.18128/D020.V7.2.

Mueller, V., Gray, C., Kosec, K., 2014. Heat stress increases long-term human migration in rural Pakistan. Nature Climate Change 4 (3), 182–185. https://doi.org/10.1038/nclimate2103.

Munshi, K., Rosenzweig, M., 2016. Networks and Misallocation: Insurance, Migration, and the Rural-Urban wage Gap. American Economic Review 106 (1), 46–98. https://doi.org/10.1257/AER.20131365.

O'Neill, B.C., Kriegler, E., Ebi, K.L., Kemp-Benedict, E., Riahi, K., Rothman, D.S., Solecki, W., 2017. The roads ahead: Narratives for shared socioeconomic pathways

describing world futures in the 21st century. Global Environ. Change 42, 169–180. https://doi.org/10.1016/j.gloenvcha.2015.01.004.
Okwi, P.O., Ndeng'e, G., Kristjanson, P., Arunga, M., Notenbaert, A., Omolo, A., Owuor, J., 2007. Spatial determinants of poverty in rural Kenya. Proc. Nat. Acad. Sci. USA 104 (43), 16769–16774. https://doi.org/10.1073/PNAS.0611107104/SUPPL_FILE/INDEX.HTML.
Opitz-Stapleton, S., Sabbag, L., Hawley, K., Tran, P., Hoang, L., Nguyen, P.H., 2016. Heat index trends and climate change implications for occupational heat exposure in Da Nang, Vietnam. Climate Services 2–3, 41–51. https://doi.org/10.1016/J.CLISER.2016.08.001.
Osberghaus, D., Abeling, T., 2022. Heat vulnerability and adaptation of low-income households in Germany. Global Environ. Change 72, 102446. https://doi.org/10.1016/j.gloenvcha.2021.102446.
Peichl, A., 2016. Linking microsimulation and CGE models. Int. J. Microsimul. 9 (1), 167–174. https://doi.org/10.34196/ijm.00132.
Pezzulo, C., Hornby, G.M., Sorichetta, A., Gaughan, A.E., Linard, C., Bird, T.J., Tatem, A. J., 2017. Sub-national mapping of population pyramids and dependency ratios in Africa and Asia. Sci. Data 4 (1), 170089. https://doi.org/10.1038/sdata.2017.89.
Piontek, F., Drouet, L., Emmerling, J., Kompas, T., Méjean, A., Otto, C., Tavoni, M., 2021. Integrated perspective on translating biophysical to economic impacts of climate change. Nature Climate Change 11 (7), 563–572. https://doi.org/10.1038/S41558-021-01065-Y.
Piontek, F., Müller, C., Pugh, T.A.M., Clark, D.B., Deryng, D., Elliott, J., Schellnhuber, H. J., 2014. Multisectoral climate impact hotspots in a warming world. Proceedings of the National Academy of Sciences 111 (9), 3233–3238. https://doi.org/10.1073/pnas.1222471110.
Pirani, A., Fuglestvedt, J.S., Byers, E., O'Neill, B., Riahi, K., Lee, J.-Y., Tebaldi, C., 2024. Scenarios in IPCC assessments: lessons from AR6 and opportunities for AR7. Npj Climate Action 3 (1), 1. https://doi.org/10.1038/s44168-023-00082-1.
Rana, I.A., Khan, M.M., Lodhi, R.H., Altaf, S., Nawaz, A., Najam, F.A., 2023. Multidimensional poverty vis-à-vis climate change vulnerability: Empirical evidence from flood-prone rural communities of Charsadda and Nowshera districts in Pakistan. World Dev. Sustainab. 2, 100064. https://doi.org/10.1016/J.WDS.2023.100064.
Randell, H., Gray, C., Grace, K., 2020. Stunted from the start: Early life weather conditions and child undernutrition in Ethiopia. Social Sci. Med. 261, 113234. https://doi.org/10.1016/J.SOCSCIMED.2020.113234.
Rao, N.D., Sauer, P., Gidden, M., Riahi, K., 2019. Income inequality projections for the Shared Socioeconomic Pathways (SSPs). Futures 105 (June 2018), 27–39. https://doi.org/10.1016/j.futures.2018.07.001.
Rao, N.D., Van Ruijven, B.J., Riahi, K., Bosetti, V., 2017. Improving poverty and inequality modelling in climate research. Nature Climate Change 7 (12), 857–862. https://doi.org/10.1038/s41558-017-0004-x.
Rentschler, J., Salhab, M., Jafino, B.A., 2022. Flood exposure and poverty in 188 countries. Nature Commun. 13 (1), 3527. https://doi.org/10.1038/s41467-022-30727-4.
Riahi, K., van Vuuren, D.P., Kriegler, E., Edmonds, J., O'Neill, B.C., Fujimori, S., Tavoni, M., 2017. The Shared Socioeconomic Pathways and their energy, land use, and greenhouse gas emissions implications: an overview. Global Environ. Change 42, 153–168. https://doi.org/10.1016/J.GLOENVCHA.2016.05.009.
Rising, J., Tedesco, M., Piontek, F., Stainforth, D.A., 2022. The missing risks of climate change. Nature 610 (7933), 643–651. https://doi.org/10.1038/s41586-022-05243-6.
Rohat, G., Wilhelmi, O., Flacke, J., Monaghan, A., Gao, J., Dao, H., van Maarseveen, M., 2019. Characterizing the role of socioeconomic pathways in shaping future urban heat-related challenges. Sci. Total Environ. 695, 133941. https://doi.org/10.1016/j.scitotenv.2019.133941.
van Ruijven, B.J., Levy, M.A., Agrawal, A., Biermann, F., Birkmann, J., Carter, T.R., Schweizer, V.J., 2014. Enhancing the relevance of shared socioeconomic pathways for climate change impacts, adaptation and vulnerability research. Climatic Change 122 (3), 481–494. https://doi.org/10.1007/S10584-013-0931-0/TABLES/1.
van Ruijven, B.J., O'Neill, B.C., Chateau, J., 2015. Methods for including income distribution in global CGE models for long-term climate change research. Energy Econ. 51, 530–543. https://doi.org/10.1016/j.eneco.2015.08.017.
Sandstad, M., Schwingshackl, C., 2022. Climate extreme indices and heat stress indicators derived from CMIP6 global climate projections. Copernicus Climate Change Service (C3S) Climate Data Store (CDS), 10.24381/cds.776e08bd.
Satoh, Y., Yoshimura, K., Pokhrel, Y., Kim, H., Shiogama, H., Yokohata, T., Oki, T., 2022. The timing of unprecedented hydrological drought under climate change. Nature Commun. 13 (1), 1–11. https://doi.org/10.1038/S41467-022-30729-2.
Schwingshackl, C., Sillmann, J., Vicedo-Cabrera, A.M., Sandstad, M., Aunan, K., 2021. Heat stress Indicators in CMIP6: estimating future trends and exceedances of impact-relevant thresholds. Earth's Future 9 (3), e2020EF001885. https://doi.org/10.1029/2020EF001885.
Sedova, B., Kalkuhl, M., Mendelsohn, R., 2019. Distributional Impacts of Weather and Climate in Rural India. Econ. Disasters Climate Change 4 (1), 5–44. https://doi.org/10.1007/S41885-019-00051-1.
Seff, I., Jolliffe, D., 2017. Multidimensional poverty dynamics in Ethiopia: how do they differ from consumption-based poverty dynamics? Ethiop. J. Econ. 25 (2), 1–35. https://doi.org/10.4314/eje.v25i2.
Soergel, B., Kriegler, E., Bodirsky, B.L., Bauer, N., Leimbach, M., Popp, A., 2021. Combining ambitious climate policies with efforts to eradicate poverty. Nature Commun. 12 (1), 1–12. https://doi.org/10.1038/s41467-021-22315-9.
SSP Database. (2016). *SSP Database (Shared Socioeconomic Pathways) - Version 1.1*. Retrieved from https://tntcat.iiasa.ac.at/SspDb.
Steadman, R. G. (1979). The assessment of sultriness. Part I: A temperature-humidity index based on human physiology and clothing Science. *Journal of Applied Meteorology and Climatology*, *18*(7), 861–873. https://doi.org/https://doi.org/10.1175/1520-0450(1979)018<0861:TAOSPI>2.0.CO;2.
Strauss, B.H., Kulp, S.A., Rasmussen, D.J., Levermann, A., 2021. Unprecedented threats to cities from multi-century sea level rise. Environ. Rese. Lett. 16 (11), 114015. https://doi.org/10.1088/1748-9326/ac2e6b.
Syrquin, M. (1988). *Chapter 7 Patterns of structural change*. https://doi.org/10.1016/S1573-4471(88)01010-1.
Tanton, R., 2014. A Review of spatial microsimulation methods. Int. J. Microsimul. 7 (1), 4–25. https://doi.org/10.34196/ijm.00092.
Tanton, R., Edwards, K.L. (Eds.), 2013. Spatial Microsimulation: A Reference Guide for Users. Springer, Netherlands, Dordrecht.
Upton, J., Constenla-Villoslada, S., Barrett, C.B., 2022. Caveat utilitor: a comparative assessment of resilience measurement approaches. J. Dev. Econ. 157, 102873. https://doi.org/10.1016/j.jdeveco.2022.102873.
Uy, T., Yi, K.M., Zhang, J., 2013. Structural change in an open economy. J. Monet Econ. 60 (6), 667–682. https://doi.org/10.1016/J.JMONECO.2013.06.002.
Vidyattama, Y., & Tanton, R. (2010). *Projecting small area statistics with Australian spatial microsimulation model (SPATIALMSM)* (No. 1; Vol. 16). Retrieved from https://www.researchgate.net/publication/267198621.
Voas, D., Williamson, P., 2001. Evaluating goodness-of-fit measures for synthetic microdata. Geogr. Environ. Modell. 5 (2), 177–200. https://doi.org/10.1080/13615930120086078.
van Vuuren, D.P., Riahi, K., Calvin, K., Dellink, R., Emmerling, J., Fujimori, S., O'Neill, B. C., 2017. The shared socio-economic pathways: trajectories for human development and global environmental change. Global Environ. Change 42, 148–152. https://doi.org/10.1016/J.GLOENVCHA.2016.10.009.
Ward, P.J., Blauhut, V., Bloemendaal, N., Daniell, J.E., de Ruiter, M.C., Duncan, M.J., Winsemius, H.C., 2020. Review article: Natural hazard risk assessments at the global scale. Nat. Hazards Earth Syst. Sci. 20 (4), 1069–1096. https://doi.org/10.5194/nhess-20-1069-2020.
Willett, W., Rockström, J., Loken, B., Springmann, M., Lang, T., Vermeulen, S., Murray, C.J.L., 2019. Food in the anthropocene: the EAT–lancet commission on healthy diets from sustainable food systems. The Lancet 393 (10170), 447–492. https://doi.org/10.1016/S0140-6736(18)31788-4.
World Bank. (2020). Poverty and Shared Prosperity 2020 : Reversals of Fortune. https://doi.org/10.1596/978-1-4648-1602-4.
World Bank. (2025). *Poverty and Inequality Platform Methodology Handbook*. Retrieved from https://datanalytics.worldbank.org/PIP-Methodology/.
World Bank. (2026). *Living Standards Measurement Study - Integrated Surveys on Agriculture (LSMS-ISA)*. Retrieved from https://www.worldbank.org/en/programs/lsms/initiatives/lsms-ISA.
WRI. (2020). *Aqueduct Floods Hazard Maps version 2*. Retrieved from https://wri-projects.s3.amazonaws.com/AqueductFloodTool/download/v2/index.html.
Ye, X., Konduri, K.C., Pendayla, R.M., Sana, B., Waddell, P., Pendyala, R.M., Waddell, P., 2009. Methodology to match distributions of both household and person attributes in generation of synthetic populations. Transportation Research Board Annual Meeting 2009.
Young, A., 2013. Inequality, the urban-rural gap, and migration. Quart. J. Econ. 128 (4), 1727–1785. https://doi.org/10.1093/QJE/QJT025.